Conf-911001--21

ANL/CP--72041

DE91 018641

FABRICATION OF OXIDE DISPERSION STRENGTHENED FERRITIC CLAD FUEL PINS*

By

L. R. Zirker & J. H. Bottcher
Fuels & Engineering Division
Argonne National Laboratory
9700 South Cass Avenue
Argonne, Illinois 60439
USA

S. Shikakura
Power Reactor & Nuclear Fuel Development Corporation
4002 Narita, Oarai-Machi, Higashi ibaraki-gun,
Ibaraki-ken, 311-13
JAPAN

C. L. Tsai
The Ohio State University
Department of Welding Engineering
190 West 19th Avenue
Columbus, OH 43210
USA

M. L. Hamilton
Pacific Northwest Laboratories
Mail Stop 8-15
P. O. Box 999
Richland, WA 99352
USA

To be presented at the
International Conference on
Fast Reactors and Related Fuel Cycles
October 28-31, 1991
Kyoto, Japan

*Work supported by the U. S. Department of Energy, Reactor Systems, Development and Technology, under Contract No. W-31-109-ENG-38

FABRICATION OF OXIDE DISPERSION STRENGTHENED FERRITIC CLAD FUEL PINS

L. R. Zirker [1]
J. H. Bottcher [2]
S. Shikakura [3]
C. L. Tsai [4]
M. L. Hamilton [5]

ABSTRACT

A resistance butt welding procedure was developed and qualified for joining ferritic fuel pin claddings to end caps. The claddings are INCO MA957 and PNC ODS lots 63DSA and 1DK1, ferritic stainless steels strengthened by oxide dispersion, while the end caps are HT9 a martensitic stainless steel. With adequate parameter control the weld is formed without a residual melt phase and its strength approaches that of the cladding. This welding process required a new design for fuel pin end cap and weld joint. Summaries of the development, characterization, and fabrication processes are given for these fuel pins.

I. INTRODUCTION

The next generation of LMRs will require long-life fuel pins with cladding that exhibit high strength and minimal swelling. Ferritic stainless steel cladding have these characteristics, but has limited creep rupture strength above 600°C[1]. Oxide dispersion strengthened (ODS) versions of ferritic stainless steels are being considered as cladding alloys possessing high temperature, high strength, and creep resistant at elevated temperatures[2,3]. Yttria is the dispersal oxide in the two alloys used in this effort, INCO MA957[4] and an alloy developed by the Power Reactor

---

1) Argonne National Laboratory,
P.O. Box 2528, Idaho Falls, Idaho, 83403-2528, USA

2) Argonne National Laboratory,
9700 South Cass Avenue, Argonne, Illinois, 60439, USA

3) Power Reactor and Nuclear Fuel Development Corporation,
4002 Narita-cho, Oarai-Machi, Higashi ibaraki-gun,
Ibaraki-ken, 311-13, JAPAN

4) The Ohio State University, Department of Welding Engineering
190 West 19th Avenue, Columbus, Ohio, 43210, USA

5) Pacific Northwest Laboratories, Mail Stop P8-15, P.O. Box
999, Richland, Washington 99352, USA

and Nuclear Fuel Development Corporation (PNC) in Japan[5]. The PNC 1DK1 cladding is to be tested in EBR-II using an advanced mixed oxide fuel pin design. It is being tested as part of a USDOE/Japan-PNC collaboration referred to as the Operational Reliability Testing Program. The MA957 cladding will also be tested in EBR-II under the auspices of the USDOE Integral Fast Reactor program, but will use mixed metal fuel pins.

These alloys achieve their elevated temperature strength and creep resistance from the finely dispersed yttria that retards recrystallization after forming. These alloys were mechanically alloyed and if fusion welded the melt and heat-affected zone (HAZ) restructuring will redistribute the yttria. A resistance butt welding process was selected on the basis of obtaining a solid state weld without recrystallization[6]. Welds from this process can be performed in a glove-box and are strong, uniform, and reproducible. This paper describes the welding development, weld characterization, and the fuel pin jacket assembly and closure welding.

II. WELD DEVELOPMENT

The advanced LMR fuel pin designs called for ODS ferritic stainless steel cladding joined to martensitic stainless steel (HT9) end plugs. The cladding size was 7.5 mm OD by 6.7 mm ID by 700-800 mm in length. The MA957 cladding was tube drawn by Superior Tube Company of the USA, and the 63DSA and 1DK1 cladding lot samples were respectively drawn by Sumitomo Metal Ind. Ltd. and Kobe Steel Ltd. of Japan. The bottom and top end plugs diameter were 7.6 mm and their respective lengths were 13 and 16 mm. Fuel pin fabrication consisted of a jacket assembly of the cladding welded to the bottom end plug and a final closure weld following fuel loading.

Welding options were limited by the morphology of the mechanically alloyed and drawn ODS material, i.e. a ferritic matrix with finely dispersed oxide particles and a highly textured microstructure. Since this morphology is responsible for the high temperature properties and any homogenization or recrystallization would be detrimental. The resistance butt welding method was selected based on a literature review and trials using friction and flash welding processes. Pulse magnetic welding has also produced quality welds[7]. All of these processes, except flash welding, have the common characteristic of forming solid state welds without fusion in a few milliseconds or less.

The equipment selected were two Voltza®Transguns designed and built by Centerline Windsor Ltd., Windsor, Ontario, Canada. Both transguns, #CLTG-9608-5 and #CLTG-9636-15 were powered by an 80 kVA transformer. The welding units were operated by a modified Square D model 3857-004-802 controller. One transgun was a "C" style, for out of glove-box use, and the other design was a scissors type that enabled welding to be performed in the glove-box more easily. These transguns are shown in Fig. 1. The key component in the design of these transguns is the patented OMHA®

cylinder used as the activator. The electrodes were modified to clamp the cladding and end plug components, and can be installed in a glove-box through a standard 23 cm glove port. The uniform loading by the electrodes was critical to the deformation welding segment of this process. In fact, the continuous uniform loading capability of the hydraulics was a principal selection factor. Equipment cost was an additional factor, particularly since this effort was supported by irradiation testing programs.

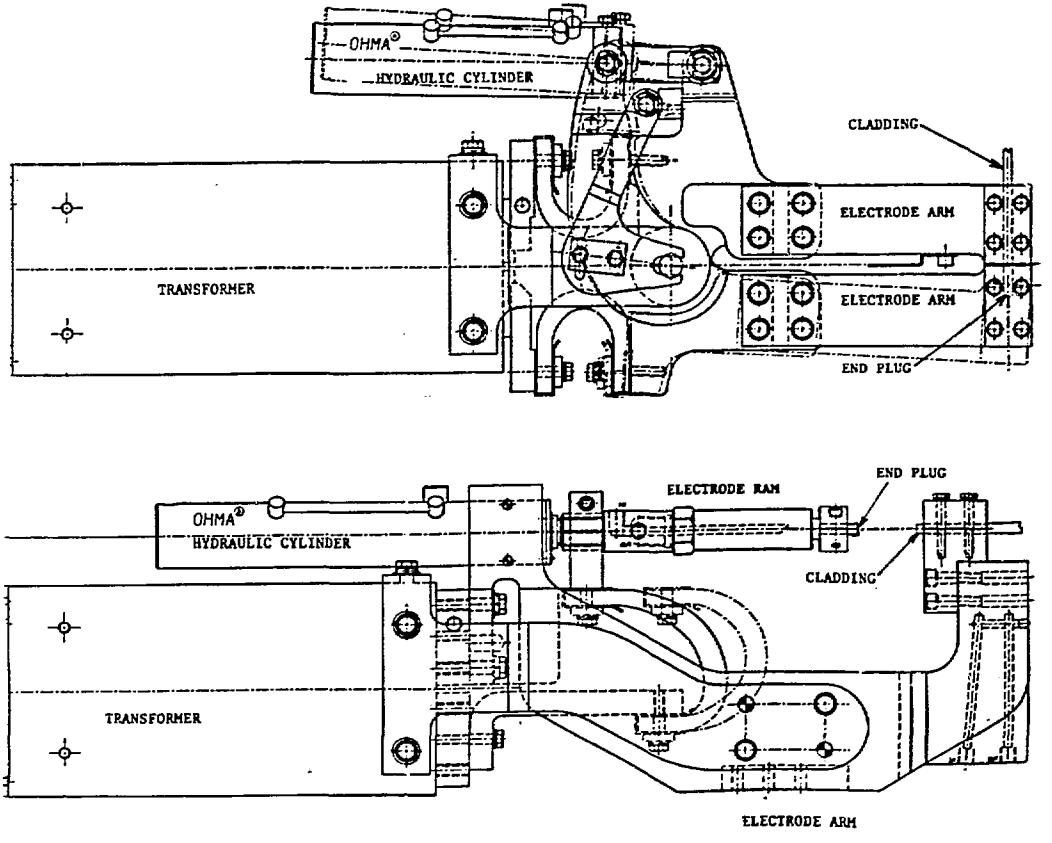

Fig. 1 Cross Sectional Drawings of Transgun Models #CLTG-9608-5 (top) and #CLTG-9636-15 (bottom).

The joint design was based on input from modeling, fuel pin design criteria, and a series of welding tests. A finite element modeling (FEM) thermal analysis[8,9] using "ANSYS" version 4.1 was used initially to identify the effect on the welding process of material property variations and specific joint design characteristics. The analysis showed that variations in either the electrical resistivity of the cladding, due to variations in

forming history, or the amount of cladding material protruding from the electrode clamps (stick-out) would significantly affect the heating profile during welding, which would impact weld quality. The final joint design consisted of the cladding butted to a right cylinder solid end plug that had a diameter approximately 0.1 mm larger than the cladding. A schematic showing the welding setup, pre-weld, and post-weld configuration are shown in Fig. 2. For the fuel pin design described above, the welding setup stick-out of the cladding and end-plug were 1.27 mm and 2.54 mm, respectively. The welding parameters were a 4.5 kN load with 11 k-amps current for 3.33×10^{-2} s.

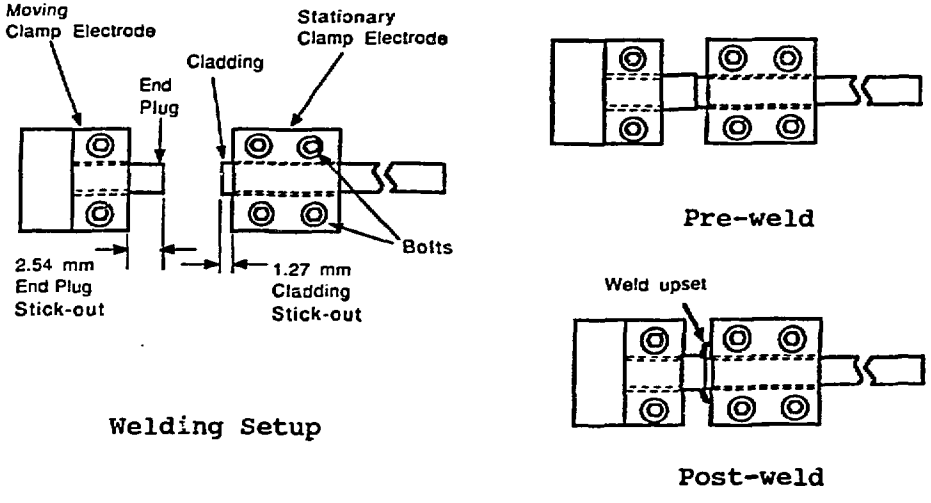

Fig. 2 Schematic of Welding Configuration.

The welding process was also analyzed thermomechanically by using an FEM analysis[10,11] run in which the elastic-plastic and transient thermal responses were coupled during the welding process. This analysis showed that the process involved two phases: an initial flash phase of a very short duration (1.5×10^{-6} s) followed by a deformation welding phase, forging. The flash stage provided heat to the relatively massive end plug and initiated the mating of both components with the expulsion of some cladding material. Figure 3 shows the temperature contour map of the weld joint just prior to material expulsion at t = 5×10^{-7} s. The peak temperature was occurring in the end of the cladding. By the end of the flash phase at t = 1.5×10^{-6} s the cladding had deformed (upset) significantly as shown in Fig. 4. The joint bonding occurred by deformation welding (forging) of the end plug and cladding butt end during the remaining portion of the time (2 cycles), $\sim 3.3 \times 10^{-2}$ s. In effect, the consistent follow up loading (4.5 kN) keeps the electrical resistance constant, thereby controlling the temperature between the cladding and end plug. A momentary decrease in loading causes very rapid resistive overheating leading to recrystallization and

grain growth or excessive expulsion. Upset during the welding cycle was ~2 mm with ~1.2 mm occurring by cladding extrusion.

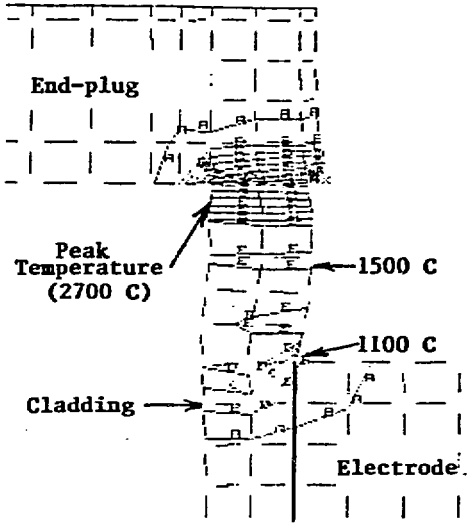

Fig. 3 Resistance welding FEM Temperature Map at $5x10^{-7}$ s.

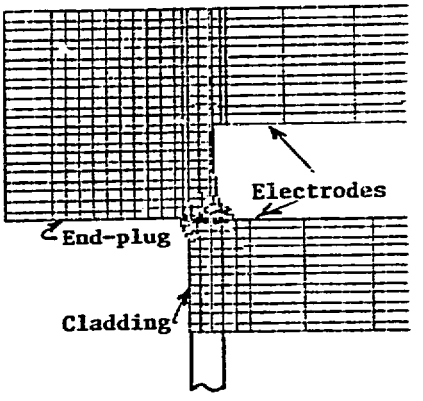

Fig. 4 Resistance Welding FEM Deformation Map at $1.5x10^{-6}$ s.

III. WELD CHARACTERIZATION

Metallographic analysis of the welds revealed a bond line that was 30% longer than the cladding wall thickness for both the MA957 and PNC claddings, see Fig. 5. The deformation flow lines were readily apparent and there was no indication of recrystallization. A preliminary SEM/EDS analysis of a polished metallographic weld sample (1DK1 cladding) verified the absence of recrystallization and also showed no discernable evidence of yttria agglomeration, migration, or any significant redistribution. Some particles in the weld seam did contain Ti and Y, which may be in the form of Y_2TiO_5.

The mechanical strength of the weld was determined by bend, tensile, and burst testing. All mechanical tests other than the bend tests were machined prior to testing to remove the upset material from the welding process. Bend testing was used primarily as a bench mark for strength and weld quality during the weld development phase of this effort, i.e. fracturing in the weld was not acceptable. The room temperature bend tests were cantilevered from the end cap and loaded at ~15 cm from the weld until failure or tube collapse. In acceptable welds, the 63DSA and 1DK1 claddings failed above the weld where as the MA957 cladding collapsed. The MA957 cladding exhibited less strength and more ductility than the PNC claddings. An example of a 1DK1 bend test failure (~5 mm above weld) is shown in Fig. 6.

Weld #C-11 32x

Weld #S-13 32x

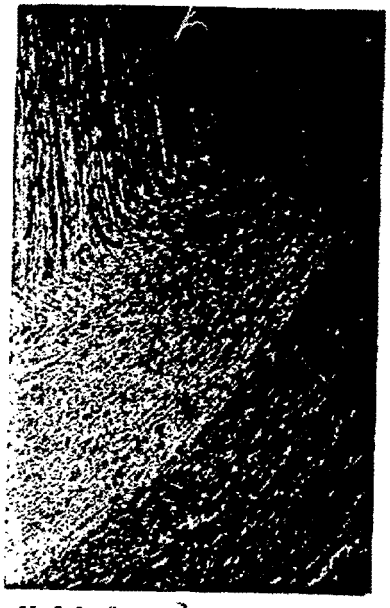

Weld #C-11 260x

Weld #S-13 260x

Fig. 5 Photomicrographs of Resistance Butt Welded 1DK (left) and MA957 (right) Cladding to HT9 End plugs.

The tensile tests were performed at room temperature by inserting a mandrel in the tubing end and straining at, 8.5×10^{-3} mm/s. Fracturing primarily occurred in the tubing with occasional propagation into the weld joint (see Fig. 6), which indicates that the weld is stronger than the cladding at the point of failure. Results of the 1DK1 cladding to HT9 end plug welds were 1200-1300 MPa yield and 1300-1400 MPa ultimate strength; the tubing strengths are 1265 and 1400 MPa, respectively. The data variance was attributed to variations in the tubing samples. The MA957 cladding is presently being tensile tested, however based on limited results the failures are also occurring in the cladding.

Biaxial burst testing was performed to verify the strength of the welds between the 1DK1 cladding and HT9 end plugs. The burst capsules were fabricated with 1DK1 tube sections (60 mm long), which due to a limited supply of cladding were first trial fabrication tube samples that were not nondestructively examined. End-plug of HT9 were welded to each end of the tube section. One end was subsequently drilled out to received inlet tubes of 304 stainless steel so that pressurization with argon could be accomplished. The specimens were tested in retorts sealed from the surrounding atmosphere with Swagelok® fittings at the inlet tubes.

Tests were performed at 550, 650, and 750°C in a flowing argon atmosphere. Capsule temperatures were monitored with chromel-alumel thermocouples (Type K). The specimens were allowed to equilibrate at the test temperature for one hour before pressurization began. The burst tests were performed by pressurizing each specimen in an increasing pressure ramp at a rate of approximately 0.5 MPa/s. Failure pressures were monitored by the motion of the needle in the pressure gage. The burst pressures are listed in Table I. The wide variance in burst pressure is assumed to be due to variations in the tubing. Failed capsules number 4, 5, and 6, are shown in Fig. 6. Biaxial creep rupture tests are being performed at the same temperatures as the burst tests.

TABLE I Burst Test Results

Capsule Number	Temperature °C	Burst Pressure, kPa	Hoop Stress, MPa
1	547	74	657
5	551	103	914
2	648	61	544
4	652	70	625
3	758	21	187
6	760	31	278

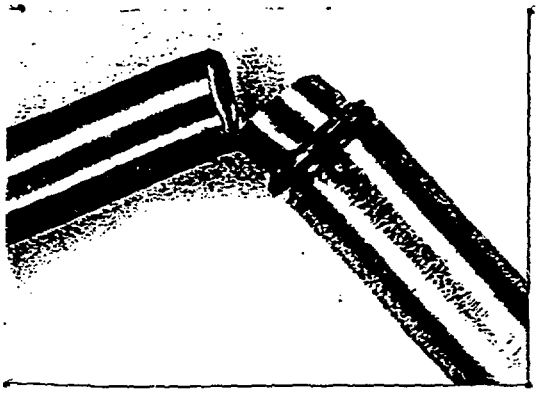

Bend Test #C-20

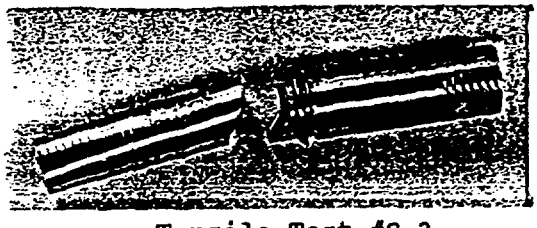

Tensile Test #S-3

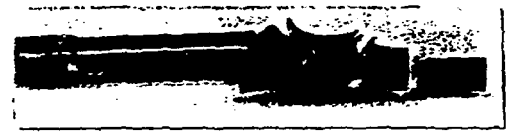

Capsule #5, 550 °C

Capsule #4, 650 °C

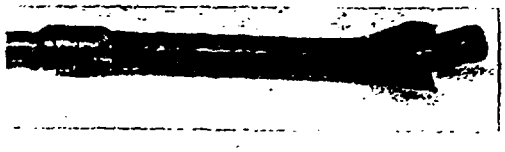

Capsule #6, 760 °C

Fig. 6 Photographs of Bend (top left), Tensile (bottom left), and Burst (right) Test Specimens.

IV. Fabrication

Fuel pin fabrication was performed in two phases: a jacket assembly and the final assembly, performed in a glove-box. The jacket comprised of cladding tube welded to the bottom end plug, which was then machined to remove the weld upset to facilitate the attachment of a grid bar adapter or spade and allow the later attachment of a wire wrap. The jacket assemblies were leak tested ($<2x10^{-9}$ cm^3/s He) and visually inspected. Data on the actual weld parameters were stored in real time as the weld was performed. This data includes the input voltage, cycles, current, percent power, and load and output voltage, current, power factor, and phase angle. In the event that the welding parameter specifications were not met an annunciator would actuate during the welding operation. Such a real time determination of the weld quality provides direct non-intrusive quality assurance[12,13].

Fuel assembly and the final closure weld were performed in a glove box. The principal factor affecting this phase of the fabrication was the space limitations. The mixed-oxide or mixed-metal was loaded and bonded, He and Na respectively. The closure welds were performed in the same manner as for the jacket. The transgun electrodes in the glove-box actuate in a scissors motion to accommodate space limitations. The quality of the closure weld

was assured by the same procedure described earlier as for the jacket weld. Each whole fuel pin was radiographed to show the weld and assure correct assembly and fuel loading.

Optional wire wrapping is performed outside of the glove-box. For ease of wire wrapping and securing the bottom end is fed through a hole in the bottom grid adapter and ball welded. The top end of wire is gas tungsten arc welded onto the top end plug.

V. Conclusions

Mixed oxide or mixed metal fuel pins can be successfully fabricated with ODS ferritic stainless steel cladding. The resistance butt welding process was proven to be both reliable and an economical method of joining the ODS cladding to a martensitic stainless steel end plug. It was crucial, however, that the load be constant during the cycle to achieve uniform deformation bonding (forging) without recrystallization.

REFERENCES

1 R. J. Puigh and F. A. Garner, "Irradiation Creep Behavior of the Fusion Heats of HT9 and Modified 9Cr-1Mo Steels," Effects of Radiation on Materials, 14th International Symposium, ASTM, Vol II, 1990, pp 527-532.

2 R. W. Powell, G. D. Johnson, M. L. Hamilton, and F. A. Gardner, "LMR Cladding and Duct Materials Development," Proceedings of International Conference on Reliable Fuels for Liquid Metal Reactors, Tucson, Az, September, 1986.

3 J. J. Huet and Ch. Lecompte, "Ferritic Steels for Fast Reactor Canning Materials and Turbine Applications," ASM International Conference on Ferritic Steels for High Temperature Applications, Warren, Pa, October, 1981

4 J. J. Fisher, U.S. Patent 4075010, "Dispersion Strengthened Ferritic Alloy for Use in Liquid Metal Fast Breeder Reactors (LMFBRs)."

5 Nomura, et al., "Development of Long Life Core Materials," Proceeding Internatioal Conference on Fast Reactor and Related Fuel Cycles, Kyoto, Japan, Oct. 28 - Nov. 1, 1991.

6 S. de Burbure, "Resistance Welding of Pressurized Capsules for In-pile Creep Experiments," Welding Journal, 33 (11), 1978.

7 W. F. Brown, J. Bandas, and N. T. Olson, "Pulse Magnetic Welding of Breeder Reactor Fuel Pin End Closures," Welding Journal, June , 1978, pp 22-26.

8 W. Rice and E. J. Funk, "An Analytical Investigation of Temperature Distributions During Resistance Welding," Welding Journal, 46 (4), 1967, pp. 175s-186s.

9 A. F. Houchens, R. E. Page, and W. H. Yang, "Numerical Modeling of Resistance Spot Welding," Numerical Modeling of Manufacturing Processes, Winter Annual Conference, ASME, Nov. 27 - Dec. 2, 1977, pp. 117-129.

10 H. A. Neid, "The Finite Element Modeling of the Resistance Spot Welding Process," Welding Journal, 64 (4), 1984, pp 123s-132s.

11 C. L. Tsai, O. A. Jammal and D. W. Dickinson, "Study of a Nugget Formation in Resistance Spot Welding Using Finite Element Method," 2nd International Conference, ASM, 14-18 May 1989, Gatlinburg, Tn.

12 W. H. Tuttle, "Improving Electronics in Arc Welding," Welding Journal, 25 (5), 1990.

13 C. L. Tsai, W. L. Dai and D. W. Dickinson, "Analysis and Development of a Real-time Control Methodology in Resistance Spot Welding," New Advances in Welding and Allied Processes, Proceedings of the International Conference, 8-10 May 1991, Beijing, China Vol. I, pp 272-278.